Supporting Information for Thermal Conductivity Reduction in Silicon Thin Film with Nanocones

X. Huang,[†] S. Gluchko,[†,‡] R. Anufriev,[†] S. Volz,[†,‡] and M. Nomura[*,†,¶]

†*Institute of Industrial Science, The Univeristy of Tokyo, Tokyo, 153-8505, Japan*

‡*Laboratory for Integrated Micro Mechatronic Systems/National Center for Scientific Research-Institute of Industrial Science (LIMMS/CNRS-IIS), The University of Tokyo, Tokyo, 153-8505, Japan*

¶*CREST, Japan Science and Technology Agency, Kawaguchi, Saitama, 332-0012, Japan*

E-mail: nomura@iis.u-tokyo.ac.jp

1 Nanocones fabrication: Inductively coupled plasma reactive ion etching (ICP-RIE)

To fabricate nanocones on 50 nm-thick silicon membrane [Figure S1(b,d)], we use an Oxford Instruments Plasmalab System100 inductively coupled plasma reactive ion etching (ICP-RIE), in which the ICP source is equipped for the generation of high-density plasma and the substrate DC bias voltage is regulated through an RF source for an excellent ion energy control.[1] We introduce SF_6 and O_2 as reactive gases and utilize the etching recipe as shown in Table 1.[2] For a better comparison of samples with and without nanocones, we also perform a standard RIE machine (Samco RIE140AI) at room temperature to etch flat silicon membrane to the same thickness of 50 nm, as shown in Figure S1(a,c).

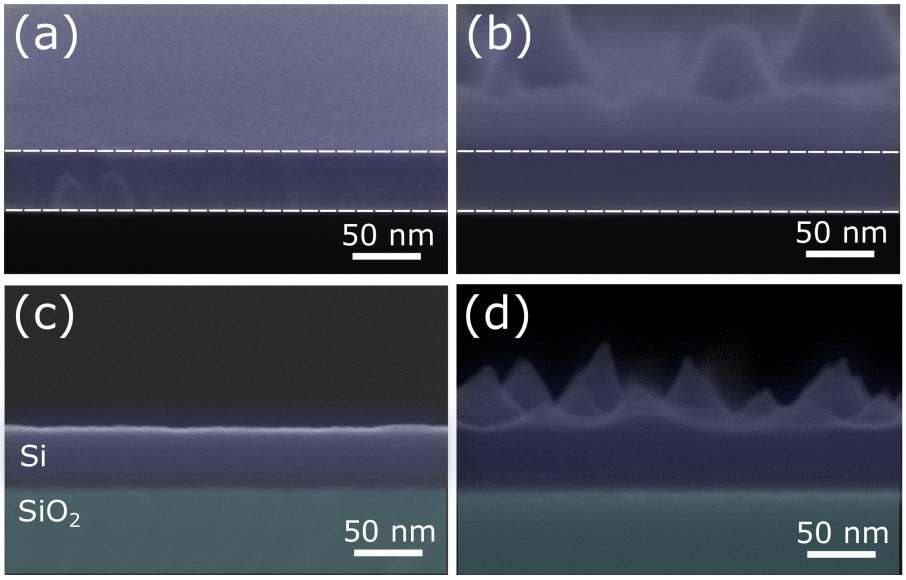

Figure S1: Tilted SEM images of membranes (a) without and (b) with nanocones after oxide layer removal. Cross-section view of membranes without (c) and with manocones before oxide layer removal (Si: purple color, SiO_2: blue color).

Table 1: Etching parameters for silicon thin films with and without nanocones

	With nanocones (ICP-RIE)	Without nanocones (RIE)
SF_6 : O_2 (sccm)	50 : 42	5 : 4
Pressure (mTorr)	34	2.25
ICP power (W)	600	0
RF power (W)	27	20
Temperature (°C)	5	20

2 Thermal properties measurement: Micro time-domain thermoreflectance (μ-TDTR) system

μ-TDTR, an all-optical system with high-speed and high-accuracy is applied for the thermal conductivity measurement in this work and the setup is illustrated by the schematic in

Figure S2(a). Samples are mounted by an Oxford Instruments cryostat with high-vacuum ($< 10^{-4}$ Pa) to avoid thermal convection, in where the temperature can be tuned from 400 K down to 3.5 K by a helium cooling system. The thermoreflectance measurements are based on the temperature dependence of a material's reflectivity,[3] as written by a simplified equation

$$\frac{\Delta R}{R} = C_{th}\Delta T \tag{1}$$

where R and ΔR are the reflectivity and its variation, C_{th} is the thermoreflectance coefficient, and ΔT is the temperature change at where the measurement laser located. Herein, aluminum is chosen as the heater/sensor since its high thermoreflectance coefficient under illumination and its strong adhesion to the underlying silicon layer.[4] First, a pulse laser with 642 nm wavelength periodically heats the sensor, the reflectivity of which raises immediately, and as heat dissipates through the structure, the reflectivity decreases gradually. Meanwhile, the change of the reflectivity is monitored by a probe laser with a wavelength of 785 nm. As can be seen in Figure S2(b), the signal has the same tendency as the temperature and follows an exponential decay curve, which can be expressed as

$$\frac{\Delta R(t)}{R} = Ae^{-t/\tau} \tag{2}$$

where A is the normalization constant, t is the time, and τ is the thermal decay time. Thus, this decay time (τ) can represent the thermal transport properties of structures on both sides of the aluminum sensor.

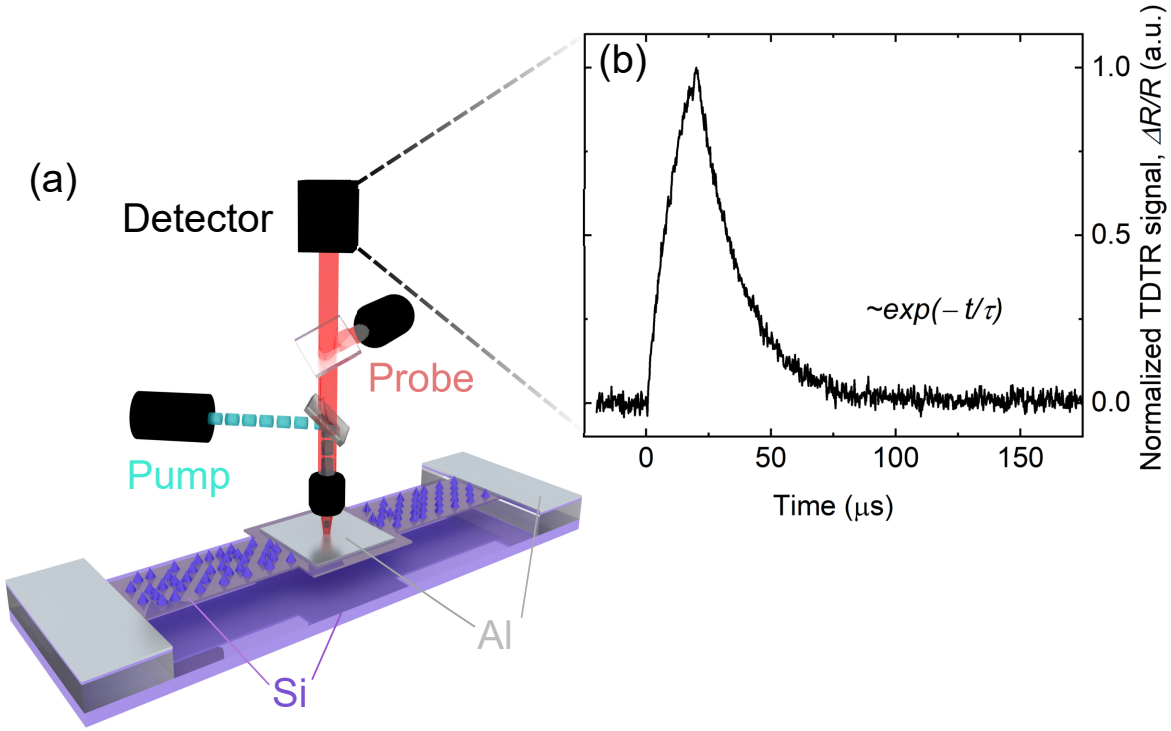

Figure S2: (a) Schematic of μ-TDTR setup. (b) Normalized thermoreflectance signal as a function of time with exponential fitting.

3 Nanocone height distribution: Atomic Force Microscope (AFM) imaging analysis

An SII NanoCute atomic force microscope (AFM) is applied in this work to obtain the morphology of the surface of the nanocone sample. Figure S3(a) shows the image of the top view of the conical structures on the silicon membrane which is scanned by a self-sensitive microcantilever (PRC-DF40P) with 20 nm-radius tips.[5] The height of the nanocones is recorded by converting the AFM image into pixels [Figure S3(b)] and locating the peaks of each cone. The height distribution of nanocones is obtained by accumulating six images with the same size of 500×500 nm^2 from different areas of one sample. Additionally, the bottom diameter of the nanocone structures is also characterized by the AFM images, which varies approximately from 50 nm to 70 nm.

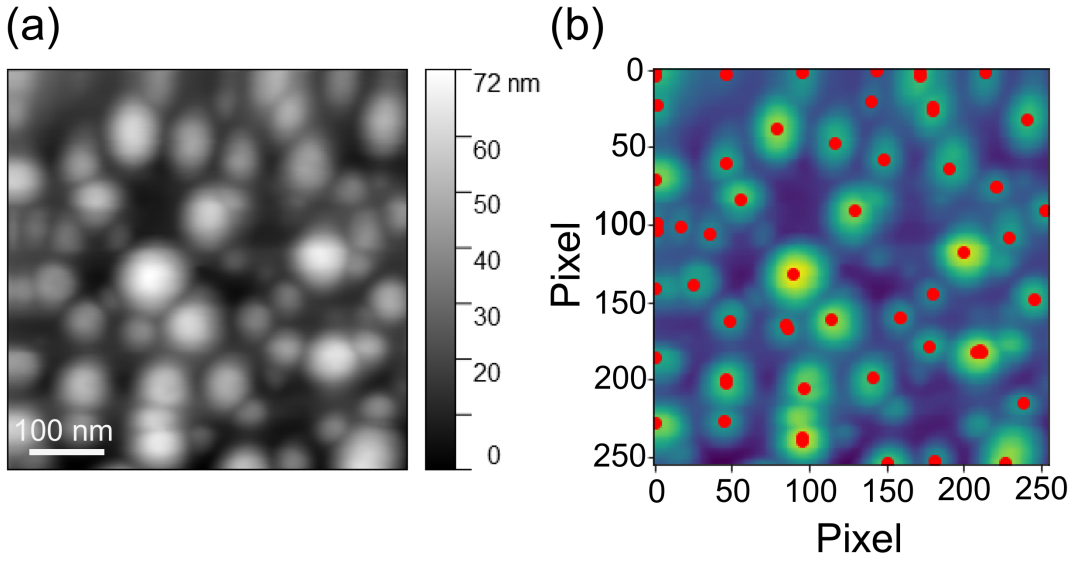

Figure S3: (a) AFM image of nanocones, and (b) its re-scaled version in pixels.

4 Thermal conductivity extraction: Finite element method (FEM) simulation by COMSOL Multiphysics

To extract the thermal conductivity, we perform simulations with FEM model using COMSOL Multiphysics®. To reproduce the same heat dissipation experiments as we did in the μ-TDTR system, we first build 3D models with the same geometries as the measured structures. The heating laser centered on the aluminum pad in the experiment is simulated by heat flux pulse with a Gaussian distribution, as shown in Figure S4(a−c).

In the simulation, the heat conduction is modeled using the heat transport equation

$$\rho C_p \frac{\partial T}{\partial t} + \nabla.(-\kappa \nabla T + \rho C_p T \mathbf{u}) = Q \tag{3}$$

where ρ is the density, C_p is the heat capacity at constant pressure, κ is the thermal conductivity, and Q is the heat sources. The thermal conductivity of the investigated structure is set as the only variable parameter. All other parameters are assumed to be equal to the values in bulk material for the temperature of interest, for example, the thermal conductivity

of both Al pad and sink is set as 237 $Wm^{-1}K^{-1}$, and the values of the heat capacity of Si and Al are 700 and 904 $Jkg^{-1}K^{-1}$ respectively at 295 K.[6,7] The thermal radiation loss of the suspended structure was estimated by Stefan-Boltzmann law and concluded to be neglected, as well as convection effect.[8] Being consistent with the experiment, the time steps should be small enough and usually set as 50−100 ns to capture the time evolution accurately. And the error produced by μ-TDTR measurement is estimated below 5−10% from our previous work,[7] such inaccuracy of the thermal conductivity data extracted by this method is less than the scale of all the effects we obtained in this work. Therefore, by sweeping a series of thermal conductivities, we can achieve their corresponding decay curves, as plotted in Figure S4(d). The accurate thermal conductivity can be obtained through the decay curve which fits our experimental data the best.[3,5]

For the membrane with nanocone structures in this work, we try to extract the effective thermal conductivity of this conical silicon material, similar to that of holey silicon used in literature. To do that, we ran the same simulation as mentioned above using membrane structure without nanocones and fit the experimental data of sample with nanocones by the simulated decay curves to obtain the correct effective thermal conductivity.[5]

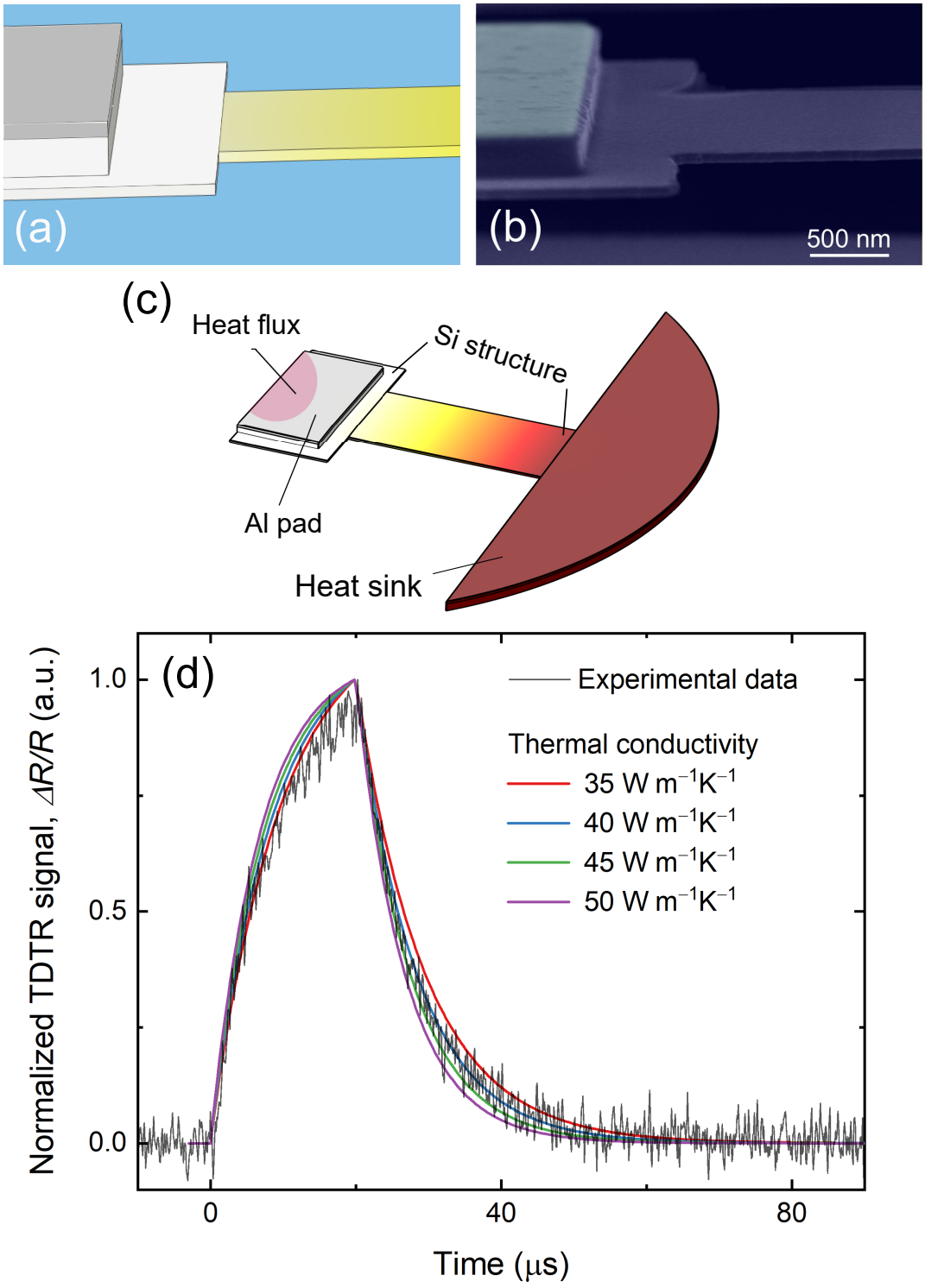

Figure S4: Details of (a) FEM model and (b) SEM of the measured structure. (c) Heat dissipation by FEM model. (d) Fitting experimental data by the decay curves from simulations with thermal conductivity as sweeping parameter.

5 Effect of surface roughness on thermal conductivity

The impact of surface roughness on thermal conductivity is evaluated using Callaway-Holland method. In the model, both surface roughness and phonon wavelength affect the specularity, contributing to the variation of thermal conductivity. Figure S5 shows that, at high temperatures, roughness does not affect thermal conductivity significantly, but which has the strongest impact at low temperatures.

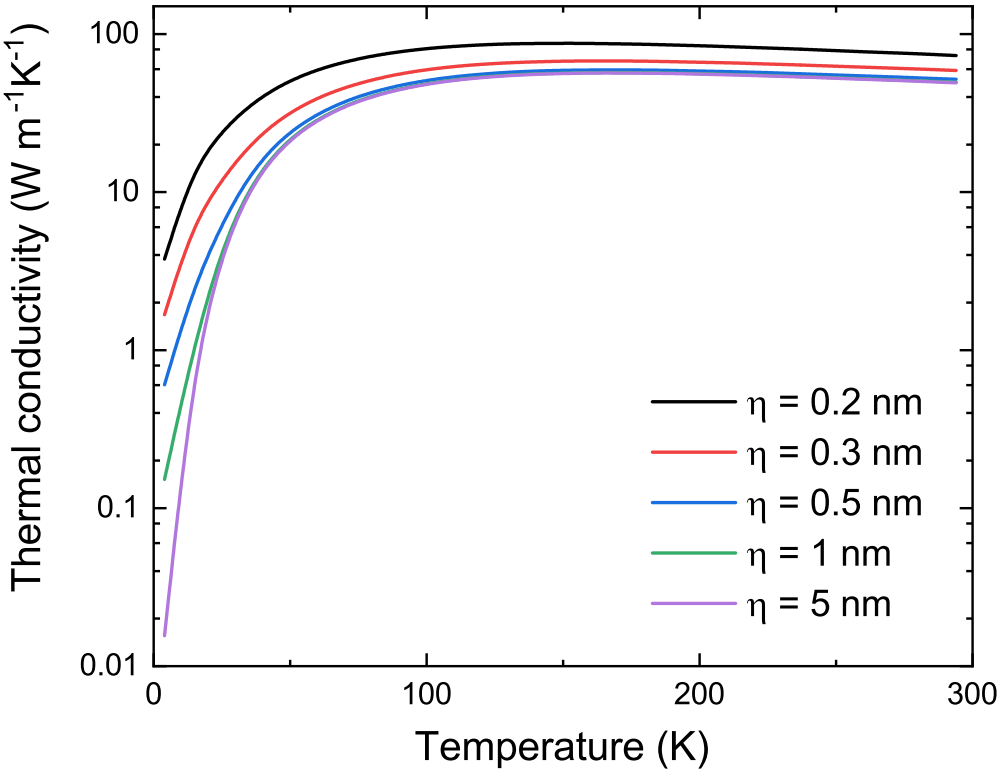

Figure S5: Thermal conductivities of 50 nm silicon membrane with different values of surface roughness (0.2, 0.3, 0.5, 1 and 5 nm) as a function of temperature. Predictions by Callaway-Holland model.

6 Thermal conductivity at low temperatures: Debye's T^3 law

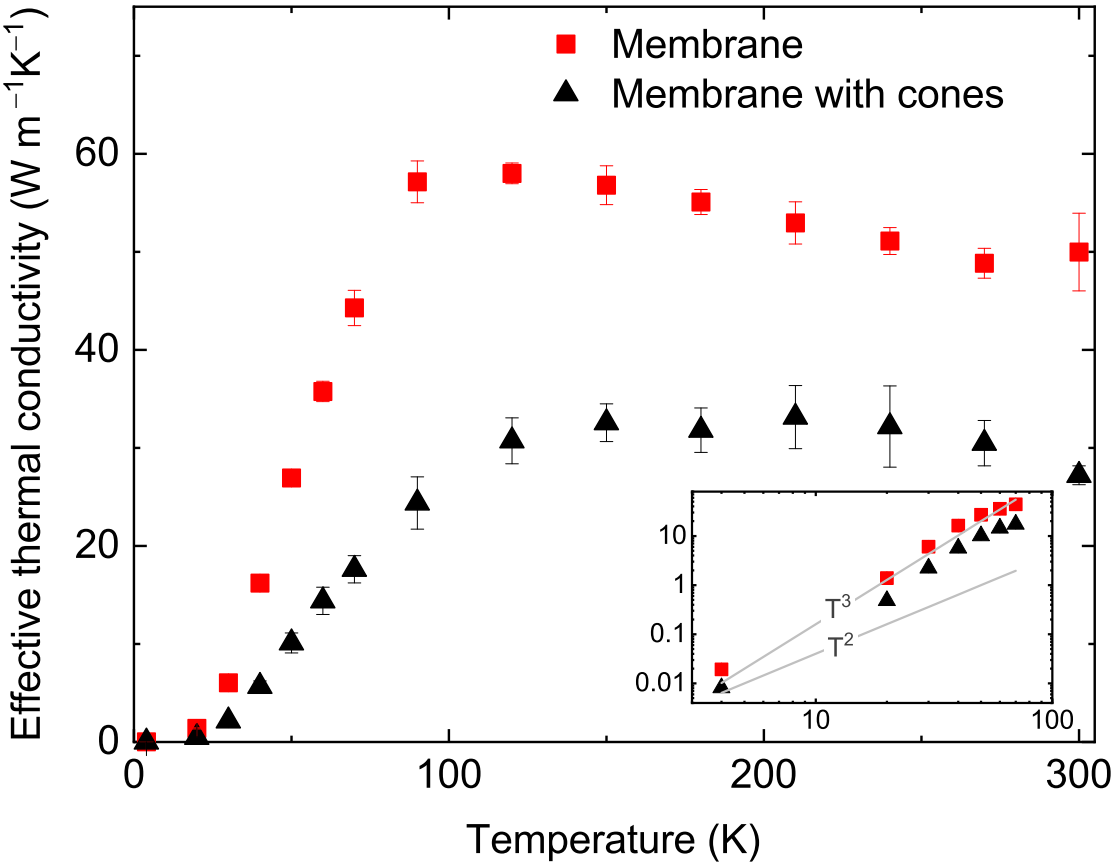

Figure S6: Effective thermal conductivity as a function of temperature for membranes with (black triangles) and without (red squares) nanocones. Inset shows at low temperatures, thermal conductivities of both two samples follow T^3 trend.

References

(1) Steglich, M.; Käsebier, T.; Zilk, M.; Pertsch, T.; Kley, E.-B.; Tünnermann, A. The structural and optical properties of black silicon by inductively coupled plasma reactive ion etching. *J. Appl. Phys.* **2014**, *116*, 173503.

(2) Gaudig, M.; Hirsch, J.; Schneider, T.; Sprafke, A. N.; Ziegler, J.; Bernhard, N.;

Wehrspohn, R. B. Properties of black silicon obtained at room-temperature by different plasma modes. *J. Vac. Sci. Technol. A* **2015**, *33*, 05E132.

(3) Maire, J. Thermal phonon transport in silicon nanosturctures. Ph.D. thesis, The University of Tokyo, 2015.

(4) Zhu, J.; Wu, X.; Lattery, D. M.; Zheng, W.; Wang, X. The Ultrafast Laser Pump-Probe Technique for Thermal Characterization of Materials With Micro/Nanostructures. *Nanoscale Microscale Thermophys. Eng.* **2017**, *21*, 177–198.

(5) Anufriev, R.; Ramiere, A.; Maire, J.; Nomura, M. Heat guiding and focusing using ballistic phonon transport in phononic nanostructures. *Nat. Commun.* **2017**, *8*, 15505.

(6) Touloukian, Y.; Powell, R.; Ho, C.; Klemens, P.; THERMOPHYSICAL,; IN., E. P. I. A. C. L. *Thermophysical Properties of Matter - The TPRC Data Series. Volume 2. Thermal Conductivity - Nonmetallic Solids*; Defense Technical Information Center, 1971.

(7) Anufriev, R.; Maire, J.; Nomura, M. Reduction of thermal conductivity by surface scattering of phonons in periodic silicon nanostructures. *Phys. Rev. B* **2016**, *93*, 045411.

(8) Nomura, M.; Kage, Y.; Nakagawa, J.; Hori, T.; Maire, J.; Shiomi, J.; Anufriev, R.; Moser, D.; Paul, O. Impeded thermal transport in Si multiscale hierarchical architectures with phononic crystal nanostructures. *Phys. Rev. B* **2015**, *91*, 205422.